

Direct Observation of Electron Dephasing due to Inelastic Scattering from Defects in Weakly Disordered AuPd Wires

Yuan-Liang Zhong,¹ Andrei Sergeev,² Chii-Dong Chen,³ and Juhn-Jong Lin^{4,*}

¹Department of Physics and Center for Nanotechnology, Chung Yuan Christian University, Chung-Li 32023, Taiwan

²Research Foundation, University at Buffalo, State University of New York, Buffalo, New York, 14260, USA

³Institute of Physics, Academia Sinica, 115 Taipei, Taiwan

⁴Institute of Physics and Department of Electrophysics, National Chiao Tung University, Hsinchu 30010, Taiwan
(Received 30 November 2009; published 20 May 2010)

To identify and investigate the mechanisms of electron-phonon (e -ph) relaxation in weakly disordered metallic conductors, we measure the electron dephasing rate in a series of suspended and supported 15-nm thick AuPd wires. In a wide temperature range, from ~ 8 K to above 20 K, the e -ph interaction dominates in the dephasing processes. The corresponding relaxation rate reveals a quadratic temperature dependence, $\tau_{e\text{-ph}}^{-1} = A_{ep}T^2$, where $A_{ep} \approx 5 \times 10^9 \text{ K}^{-2} \text{ s}^{-1}$ is essentially the same for all samples studied. Our observations are shown to be in good agreement with the theory which predicts that, even in weakly disordered metallic structures at moderately low temperatures, the major mechanism of the e -ph relaxation is the electron scattering from vibrating defects and impurities.

DOI: 10.1103/PhysRevLett.104.206803

PACS numbers: 73.23.-b, 63.20.K-, 71.36.+c, 72.15.Rn

In pure bulk metals the electron-phonon (e -ph) interaction is due to deformations, which modify the local charge distribution and cause electron scattering from the local charge [1,2]. In disordered metals and metallic nanostructures, inelastic electron scattering from vibrating impurities, defects, and boundaries generates an additional channel of the e -ph interaction [3]. Recently, significant experimental research [4–8] has been focused on the e -ph relaxation in the diffusive limit, $q_T\ell < 1$ ($q_T = k_B T/\hbar u$ is the wave number of a thermal phonon, u is the sound velocity, and ℓ is the electron mean free path), where these two mechanisms interfere and the net e -ph relaxation may be suppressed [2,9] or enhanced [3], depending sensitively on the vibrations of electron scatterers.

In the opposite, quasiballistic limit, $q_T\ell > 1$, these two e -ph scattering mechanisms are additive. The well-developed theory [3,9] predicts that in a wide temperature range,

$$T^* = \frac{\hbar u_t}{k_B \ell} \leq T \leq \frac{6\pi}{7\zeta(3)} \left(\frac{u_l}{u_t}\right)^4 \frac{\hbar u_l}{k_B \ell} \approx 35T^*, \quad (1)$$

electron scattering from vibrating defects and impurities provides the main contribution to the e -ph relaxation rate,

$$\frac{1}{\tau_{e\text{-t.ph}}} = \frac{3\pi^2 k_B^2 \beta_t T^2}{(p_F u_t)(p_F \ell)}. \quad (2)$$

Here β_t is the electron-transverse phonon coupling constant, p_F is the Fermi momentum, and u_t (u_l) is the transverse (longitudinal) sound velocity. Note that Eq. (2) is derived within the Pippard model, which assumes that defects and impurities vibrate in phase with host ions, so their scattering potentials are accounted for via ℓ . The transverse modes are substantially softer than longitudinal ones (i.e., u_l/u_t is typically ≥ 2), and hence they play a

leading role in the e -ph relaxation via vibrating impurities and defects [Eq. (2)].

The impurity or defect-induced e -ph relaxation [Eq. (2)] is expected to be seen in a wide temperature interval [Eq. (1)]. However, previous experiments had mostly been focused on relatively low temperatures and relatively disordered materials [10–15]. The observed temperature dependencies of the e -ph relaxation rate close to T^3 , weak dependencies of relaxation on ℓ , and absolute values of $\tau_{e\text{-ph}}^{-1}$ are in good agreement with the theory [9,16] and correspond to the crossover of the electron-transverse phonon relaxation rate changing from a T^2/ℓ dependence [Eq. (2)] to a $T^4\ell$ dependence in the diffusive limit [17]. At the same time, most experimental papers associate such dependencies with the relaxation derived for pure bulk metals, i.e., with $\tau_{e\text{-l.ph}}^{-1} \propto T^3\ell^0$, but cannot explain the large values of relaxation rate.

To clarify the role of defects and impurities in the e -ph relaxation, which has been theoretically addressed for decades [2,3,9,16], but has not been experimentally studied thus far, we investigate the dephasing rate in relatively pure AuPd wires in a wide temperature range under conditions of the quasiballistic limit.

We have studied the e -ph relaxation in a series of suspended (freestanding) and supported 15-nm thick AuPd narrow and wide wires. Suspended AuPd wires as well as AuPd on suspended SiO_2 membrane (denoted as AuPd/ SiO_2) wires were fabricated by electron beam lithography. Thin $\text{Au}_{50}\text{Pd}_{50}$ (molar concentration) films were thermally evaporated onto either silicon-on-insulator (SOI) substrates or a SiO_2 layer (30 nm thick) capped SOI substrates. The films were patterned into wires with different widths. In both types of suspended thin wire structures, the Si layer in the SOI substrate was removed by reactive

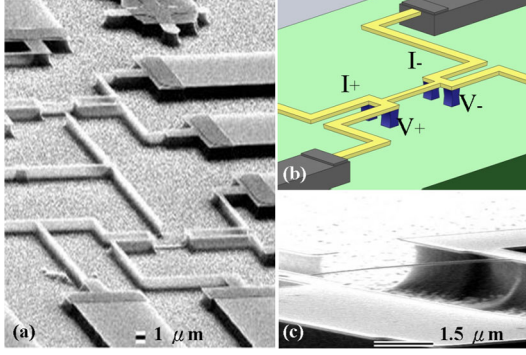


FIG. 1 (color online). (a) An SEM image for two suspended AuPd wires with freestanding current and voltage leads, (b) a schematic diagram depicting our suspended four-probe wire structure, and (c) an SEM image of a close-up of an individual suspended AuPd wire.

ion etching with a gas mixture of CF_4 and O_2 [18]. Isotropic etching of the Si layer resulted in freestanding AuPd [Fig. 1(c)] and AuPd/ SiO_2 wires. A scanning electron microscope (SEM) image for a suspended four-probe configuration is shown in Fig. 1(a), together with a schematic diagram depicted in Fig. 1(b). For complementary studies, we also fabricated four supported AuPd wires on SiO_2 substrates. The length of our wires was $4 \mu\text{m}$, while the width varied from 30 to 580 nm. The parameters of our samples are listed in Table I.

We have measured weak-localization (WL) effects in the magnetoresistance (MR) of our wires in a perpendicular magnetic field below 1 T. Small measuring currents ($\leq 10 \text{ nA}$) allowed us to avoid Joule heating. Figure 2(a) shows the normalized MRs, $\Delta R(B)/R(0) = [R(B) - R(0)]/R(0)$, at various temperatures for the representative 1D2 wire, while Fig. 2(b) shows the normalized $\Delta R_{\square}(B)/R_{\square}^2(0) = [R_{\square}(B) - R_{\square}(0)]/R_{\square}^2(0)$ for the representative 2D1S wire (R_{\square} is the sheet resistance). In all samples, the MRs are positive due to strong spin-orbit scattering [19,20]. In this case, the dependence $\Delta R(B)$ or $\Delta R_{\square}(B)$ is fully described by one adjustable parameter, the electron dephasing time τ_{φ} . To determine τ_{φ} , the MRs of

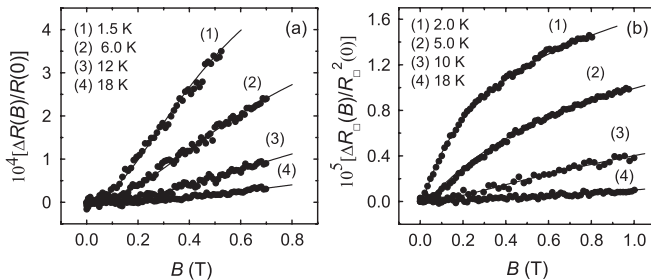


FIG. 2. Normalized MR as a function of perpendicular magnetic field for the (a) 1D2 and (b) 2D1S wires at four temperatures, as indicated. The solid curves in (a) and (b) are least-squares fits to the 1D and 2D WL theories, respectively.

each sample were fitted by the one- or two-dimensional WL theory, according to the sample's dimensionality with regard to the WL effect [20,21]. Figure 3 shows dependences $\tau_{\varphi}(T)$ for representative samples, as indicated. (We have used the diffusion constant $D = 606/\rho \text{ cm}^2/\text{s}$ [19], where ρ is the residual resistivity in units of $\mu\Omega \text{ cm}$.)

The e -ph relaxation time can then be extracted from τ_{φ} according to the following equation:

$$\frac{1}{\tau_{\varphi}(T)} = \frac{1}{\tau_0} + \frac{1}{\tau_{e-e}(T)} + \frac{1}{\tau_{e\text{-ph}}(T)}, \quad (3)$$

where τ_0 is a constant, whose origins are a subject of elaborate investigations [21–24]. The electron-electron (e - e) relaxation time, τ_{e-e} , in low-dimensional disordered conductors is well understood. We use the standard expression: $\tau_{e-e}^{-1} = A_{ee}T^n$, where $n = 2/3$ and 1 in one- and two-dimensional samples, with respect to the e - e interaction effect [5,25]. The e -ph relaxation rate was fitted in the form $\tau_{e\text{-ph}}^{-1} = A_{ep}T^p$. As it is shown in Fig. 3, the dependencies τ_{φ} are well fitted by Eq. (3) with four adjustable parameters τ_0 , A_{ee} , A_{ep} , and p . Values of A_{ee} listed in Table I are in line with those previously measured in AuPd samples [24] as well as in agreement with the theoretical predictions to within a factor of 2 to 3 [25]. Values of $p = 2.0 \pm 0.15$ and $A_{ep} \approx 5 \times 10^9 \text{ K}^{-2} \text{ s}^{-1}$ have been found to be essentially the same for all our samples. It is important to stress that even at 8 K the contribution of the e - e interaction to the dephasing rate does not exceed 6% and rapidly decreases at higher temperatures. Thus, above 8 K the temperature dependent dephasing rate is predominantly

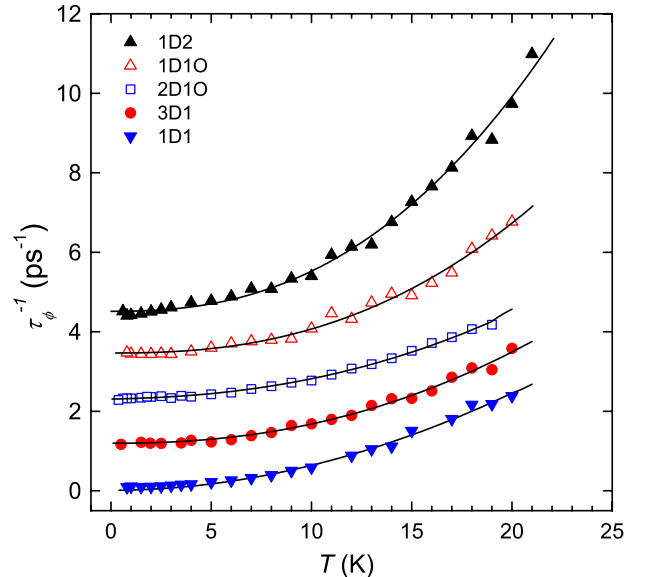


FIG. 3 (color online). Electron dephasing rate as a function of temperature for five samples, as indicated. The solid curves are least-squares fits to Eq. (3). For clarity, the τ_{φ}^{-1} of the 3D1, 2D10, 1D10, and 1D2 samples have been vertically shifted up by 1, 2, 3, and 4 ps^{-1} , respectively.

TABLE I. Values for relevant parameters of AuPd samples. $d = 15$ nm for all samples, except the 3D1. w is the width. R_{\square} is the sheet resistance at 10 K. A_{ee} is the measured strength of τ_{e-e}^{-1} . $n = 2/3$ (1) in 1D (2D). Type A stands for supported AuPd wires, type B for suspended AuPd wires, and type C for suspended AuPd/SiO₂ wires. Sample 3D1 is taken from Ref. [19], which has the same molar concentration Au₅₀Pd₅₀ and was fabricated via dc sputtering. It is 1.0 mm wide and 512 nm thick, with resistivity $\rho(10\text{ K}) = 71.4\ \mu\Omega\text{ cm}$.

Wire	Type	w (nm)	R_{\square} (Ω)	τ_0^{-1} (s^{-1})	A_{ee} ($\text{K}^{-n}\text{ s}^{-1}$)
1D1	A	30	47.5	8.0×10^{10}	7.4×10^9
1D2	A	65	31.2	4.4×10^{11}	4.7×10^9
1D1S	B	66	32.0	4.4×10^{11}	5.2×10^9
1D1O	C	37	49.0	4.0×10^{11}	4.2×10^9
2D1	A	470	22.6	3.0×10^{10}	1.4×10^8
2D2	A	200	29.2	4.4×10^{11}	8.8×10^8
2D1S	B	400	63.4	1.5×10^{10}	1.1×10^9
2D2S	B	250	23.1	3.2×10^{11}	3.8×10^8
2D1O	C	580	26.4	3.1×10^{11}	8.3×10^8
3D1	(bulk)	1.3×10^{11}	...

determined by the e -ph interaction, which provides a T^2 relaxation rate in all suspended and supported weakly disordered AuPd wires. These observations are summarized in Fig. 4, which presents a robust quadratic temperature behavior of $\tau_{e\text{-ph}}^{-1}$ (the main panel, where the solid lines plot our least-squares fitted $A_{ep}T^p$) and values of A_{ep} (inset) for various samples.

Now let us compare our observations with the theory. In AuPd alloy, $u_t \approx 1300$ m/s and $u_l \approx 3500$ m/s. Furthermore, we have utilized the thermal evaporation deposition method so that $\ell \approx 1.5$ nm is moderately long, and the dimensionless parameter $q_t\ell \equiv (k_B T / \hbar u_t)\ell \approx 0.15T$ (where T is in K). This value of $q_t\ell$ suggests that when $T \geq 6$ K, our samples fall within the quasiballistic limit, and a quadratic temperature dependence is to be expected in a wide temperature interval [Eq. (1)]. Indeed, this is exactly what we have observed in Fig. 4, where the T^2 temperature dependence is evident from ~ 8 K to above 20 K, as discussed. (The WL MRs became too small to be accurately measured at temperatures much above 20 K.) To the best of our knowledge, this is the first experimental observation of the e -ph relaxation via vibrating defects and impurities in the quasiballistic limit over a meaningfully wide range of temperature.

In contrast, it should be noted that the quadratic temperature behavior of $\tau_{e\text{-ph}}^{-1}$ previously observed in many disordered metallic alloys in the diffusive regime [5–7] is due to constructive interference of electron scattering mechanisms. There the electron-transverse phonon relaxation is enhanced (as compared with the Pippard ineffectiveness condition, $\tau_{e\text{-ph}}^{-1} \propto T^4\ell$ [2,9]), owing to the vital factor that vibrations of defects and impurities differ from vibrations of host atoms [3,26].

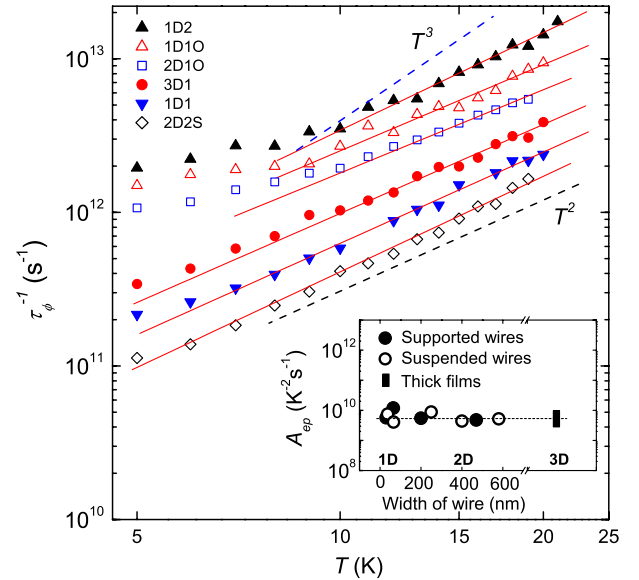


FIG. 4 (color online). $\log\tau_{e\text{-ph}}^{-1}$ versus $\log T$ for six samples, as indicated. The straight solid lines are the least-squares fitted $\tau_{e\text{-ph}}^{-1} = A_{ep}T^p$. For clarity, the $\tau_{e\text{-ph}}^{-1}$ of the 1D2, 1D1O and 2D1O wires have been vertically shifted up by multiplying a factor of 2.5, while the $\tau_{e\text{-ph}}^{-1}$ of the 3D1 sample has been vertically shifted up by multiplying a factor of 1.5. Inset: Least-squares fitted values of A_{ep} . The dashed line is a guide to the eye.

The T^2 -relaxation rate, which at first glance could be associated with Eq. (2), was reported in Ref. [27]. It was extracted from the thermal resistances measured in 10- and 100-nm thick CuCr films at 0.5–10 K. According to evaluations in Ref. [27], in this temperature range in the 10-nm films the parameter $q_T\ell$ varies from 0.1 to 1.9, which falls mainly into the diffusive limit, while in the 100-nm films, $q_T\ell$ varies from 1.1 to 21, which corresponds to the quasiballistic limit. Despite this principal difference, the same relaxation rate has been observed in 10- and 100-nm films. For these reasons, the authors of [27] concluded that their observations cannot be described by the Pippard model and associated the relaxation with the ordinary interaction between electrons and quasi-2D surface and/or grain boundary effects.

We would like also to note that numerous investigations of superconducting transition edge detectors show that in 100-nm thick films the bolometric effect, i.e., heating of the film phonons with respect to the substrate, dominates significantly over the electron heating with respect to the film phonons [16,28]. Thus, at liquid-helium temperatures in such thick films the thermal boundary resistance prevails over the e -ph thermal resistance and, therefore, explanation of the relaxation in terms of the e -ph relaxation is questionable. Strictly speaking, investigations of the quasiballistic limit over a substantial temperature range with steady-state heating measurements require ultrathin and, simultaneously, very pure films. The relaxation in such films is still unexplored. Direct measurements of the re-

laxation rate, i.e., transient response measurements, require high responsivity to the electron heating and are limited by superconducting films at the transition temperature [28]. For these reasons, in the quasiballistic limit investigations of e -ph processes via electron dephasing have substantial advantages over heating measurements.

Let us now compare our experimental values of A_{ep} with the theoretical prediction of Eq. (2). To evaluate the interaction constant $\beta_l = (\frac{2}{3}E_F)^2 N(0)/(2\rho_m u_l^2)$, we use the following parameters from Ref. [29] for Au₅₀Pd₅₀ alloy: the Fermi energy $E_F \approx 7.5$ eV, the electronic density of states at the Fermi level $N(0) \approx 2 \times 10^{47}$ states/J m³, and the mass density $\rho_m \approx 1.6 \times 10^4$ kg/m³. This evaluation gives $\beta_l \approx 2.4$. Note that this value of β_l is in reasonable agreement with the evaluation based on the Bohm-Staver relation, $(u_l/v_F)^2 = Zm/3M$, where M is the mass of the ion and Z is the number of conduction electrons per atom [30]. The Bohm-Staver relation leads to the electron-longitudinal phonon coupling constant $\beta_l = 0.5$ [2], so β_l may be computed as $\beta_l = \beta_l(u_l/v_F)^2 \approx 3.6$. Finally, substituting $\beta_l = 2.4$ and $p_F \approx 1.9 \times 10^{-24}$ kg m/s into Eq. (2) and calculating A_{ep} , we obtain 2×10^9 K⁻² s⁻¹, which is in satisfactory agreement with our experimental value of $A_{ep} \approx 5 \times 10^9$ K⁻² s⁻¹.

In summary, we have measured the e -ph relaxation time in a series of suspended as well as supported AuPd thin wires. We have found a characteristic relaxation rate $\tau_{e-ph}^{-1} \propto T^2$ for a range of temperature from ~ 8 K to above 20 K. This inelastic rate manifests a direct observation of the e -ph relaxation via electron scattering on vibrating defects. Our results reveal overall agreement with theory, according to which the transverse phonons (transverse vibrations of defects) provide the main contribution to this relaxation mechanism.

This work was supported by Taiwan NSC through Grant No. 98-2112-M-033-005 (Y.L.Z.) and No. 98-2120-M-009-004 (J.J.L.), and by the MOE ATU Program (J.J.L.). Research of A.S. was supported by NSF under Grant No. DMR 0907126.

*jjlin@mail.nctu.edu.tw

- [1] C. Kittel, *Quantum Theory of Solids* (Wiley, New York, 1963), p. 326.
- [2] B. Pippard, *Philos. Mag.* **46**, 1104 (1955).
- [3] A. Sergeev and V. Mitin, *Phys. Rev. B* **61**, 6041 (2000).
- [4] J.T. Karvonen and I.J. Maasilta, *Phys. Rev. Lett.* **99**, 145503 (2007).
- [5] J.J. Lin and J.P. Bird, *J. Phys. Condens. Matter* **14**, R501 (2002).
- [6] J.J. Lin and C.Y. Wu, *Europhys. Lett.* **29**, 141 (1995); C.Y. Wu, W.B. Jian, and J.J. Lin, *Phys. Rev. B* **57**, 11 232 (1998); A.K. Meikap, Y.Y. Chen, and J.J. Lin, *ibid.* **69**, 212202 (2004); L. Li, S.T. Lin, C. Dong, and J.J. Lin, *ibid.* **74**, 172201 (2006).
- [7] R. Ceder, O. Agam, and Z. Ovadyahu, *Phys. Rev. B* **72**, 245104 (2005).
- [8] M.E. Gershenson, D. Gong, T. Sato, B.S. Karasik, and A.V. Sergeev, *Appl. Phys. Lett.* **79**, 2049 (2001).
- [9] J. Rammer and A. Schmid, *Phys. Rev. B* **34**, 1352 (1986).
- [10] M.L. Roukes, M.R. Freeman, R.S. Germain, R.C. Richardson, and M.B. Ketchen, *Phys. Rev. Lett.* **55**, 422 (1985).
- [11] B.J. Dalrymple, S.A. Wolf, A.C. Ehrlich, and D.J. Gillespie, *Phys. Rev. B* **33**, 7514 (1986).
- [12] C.S. Yung, D.R. Schmidt, and A.N. Cleland, *Appl. Phys. Lett.* **81**, 31 (2002).
- [13] F.C. Wellstood, C. Urbina, and J. Clarke, *Phys. Rev. B* **49**, 5942 (1994).
- [14] M. Kamskar and M.N. Wybourne, *Phys. Rev. Lett.* **73**, 2123 (1994).
- [15] A. Stolovits, A. Sherman, R.K. Kremer, H. Mattausch, H. Okudera, X.M. Ren, A. Simon, and J.R. O'Brien, *Phys. Rev. B* **71**, 144519 (2005).
- [16] A. Sergeev and M. Reizer, *Int. J. Mod. Phys. B* **10**, 635 (1996).
- [17] A. Sergeev, B. Karasik, M. Gershenson, and V. Mitin, *Physica (Amsterdam)* **316–317B**, 328 (2002).
- [18] A.N. Cleland, *Foundations of Nanomechanics* (Springer, Berlin, 2003).
- [19] Y.L. Zhong and J.J. Lin, *Phys. Rev. Lett.* **80**, 588 (1998).
- [20] J.J. Lin and N. Giordano, *Phys. Rev. B* **35**, 545 (1987).
- [21] F. Pierre, A.B. Gougam, A. Anthore, H. Pothier, D. Esteve, and N.O. Birge, *Phys. Rev. B* **68**, 085413 (2003).
- [22] P. Mohanty, E.M.Q. Jariwala, and R.A. Webb, *Phys. Rev. Lett.* **78**, 3366 (1997).
- [23] J.J. Lin and N. Giordano, *Phys. Rev. B* **35**, 1071 (1987); S.M. Huang, T.C. Lee, H. Akimoto, K. Kono, and J.J. Lin, *Phys. Rev. Lett.* **99**, 046601 (2007).
- [24] D. Natelson, R.L. Willett, K.W. West, and L.N. Pfeiffer, *Phys. Rev. Lett.* **86**, 1821 (2001).
- [25] B.L. Altshuler, A.G. Aronov, M.E. Gershenson, and Yu.V. Sharvin, *Sov. Sci. Rev., Sect. A* **9**, 223 (1987).
- [26] A. Sergeev and V. Mitin, *Europhys. Lett.* **51**, 641 (2000).
- [27] J.F. DiTusa, K. Lin, M. Park, M.S. Isaacson, and J.M. Parpia, *Phys. Rev. Lett.* **68**, 1156 (1992).
- [28] A.D. Semenov, G. N. Gol'tsman, and R. Sobolewski, *Supercond. Sci. Technol.* **15**, R1 (2002).
- [29] P. Weinberger, R. Dirl, A.M. Boring, A. Gonis, and A.J. Freeman, *Phys. Rev. B* **37**, 1383 (1988).
- [30] D. Bohm and T. Staver, *Phys. Rev.* **84**, 836 (1951).